

Measurement of CP Violation in the Decay $B^+ \rightarrow K^+ \pi^0$

R. Aaij *et al.*^{*}
(LHCb Collaboration)



(Received 23 December 2020; accepted 28 January 2021; published 2 March 2021; corrected 4 March 2021)

A measurement of CP violation in the decay $B^+ \rightarrow K^+ \pi^0$ is reported using data corresponding to an integrated luminosity of 5.4 fb^{-1} collected with the LHCb experiment at a center-of-mass energy of $\sqrt{s} = 13 \text{ TeV}$. The CP asymmetry is measured to be $0.025 \pm 0.015 \pm 0.006 \pm 0.003$, where the uncertainties are statistical, systematic, and due to an external input. This is the most precise measurement of this quantity. It confirms and significantly enhances the observed anomalous difference between the direct CP asymmetries of the $B^0 \rightarrow K^+ \pi^-$ and $B^+ \rightarrow K^+ \pi^0$ decays, known as the $K\pi$ puzzle.

DOI: 10.1103/PhysRevLett.126.091802

Rare decays of heavy flavored hadrons that primarily proceed through loop-level transitions are powerful probes of the effects of new physics (NP) beyond the Standard Model (SM). The family of $B \rightarrow K\pi$ decays is dominated by hadronic loop amplitudes in the SM, but include contributions from suppressed tree-level processes, as well as electroweak loop-level processes through which NP may affect the decay [1–4]. Studies of the decay $B^0 \rightarrow K^+ \pi^-$ at the B -factory experiments led to the first observation of direct CP violating asymmetries in the B system [5,6] resulting from the interference of two decay amplitudes where both the relative strong and weak phases are non-zero. The observed asymmetries in these modes are a result of the interference between tree- and loop-level amplitudes. Further studies at the B -factory and Tevatron experiments and at LHCb have provided measurements of the branching fractions and CP asymmetries of the complete set of $B \rightarrow K\pi$ decays: $B^0 \rightarrow K^+ \pi^-$ [7–10], $B^+ \rightarrow K^+ \pi^0$ [8,11], $B^0 \rightarrow K^0 \pi^0$ [12,13], and $B^+ \rightarrow K^0 \pi^+$ [8,14,15], where the inclusion of charge-conjugated processes is implied throughout this Letter, except where asymmetries are discussed. The amplitudes in the SM are expected to obey relations imposed by isospin symmetry [1–4,16–21]. However, measurements have revealed inconsistencies with this expectation. The largest observed discrepancy is between the measured direct CP asymmetries of the decays $B^0 \rightarrow K^+ \pi^-$ and $B^+ \rightarrow K^+ \pi^0$. The difference between $A_{CP}(B^0 \rightarrow K^+ \pi^-) = -0.084 \pm 0.004$ and $A_{CP}(B^+ \rightarrow K^+ \pi^0) = 0.040 \pm 0.021$ is nonzero at 5.5 standard deviations (σ), whereas equal asymmetries are expected based on

isospin arguments. A more accurate examination of this anomaly, known as the $K\pi$ puzzle, is through the sum rule

$$\begin{aligned} A_{CP}(K^+ \pi^-) + A_{CP}(K^0 \pi^+) \frac{\mathcal{B}(K^0 \pi^+)}{\mathcal{B}(K^+ \pi^-)} \frac{\tau_0}{\tau_+} \\ = A_{CP}(K^+ \pi^0) \frac{2\mathcal{B}(K^+ \pi^0)}{\mathcal{B}(K^+ \pi^-)} \frac{\tau_0}{\tau_+} + A_{CP}(K^0 \pi^0) \frac{2\mathcal{B}(K^0 \pi^0)}{\mathcal{B}(K^+ \pi^-)}, \end{aligned} \quad (1)$$

proposed in Ref. [19], where $A_{CP}(K\pi)$ and $\mathcal{B}(K\pi)$ are the CP asymmetries and the branching fractions of the $B \rightarrow K\pi$ decays and τ_0/τ_+ is the ratio of the B^0 and B^+ lifetimes. This sum rule predicts a nonzero direct asymmetry of $A_{CP}(B^0 \rightarrow K^0 \pi^0) = -0.150 \pm 0.032$ using current world averages for the other quantities [22]. The current measurement of this quantity is 0.01 ± 0.10 [22]. The $K\pi$ puzzle has been the subject of significant theoretical attention, which includes more complete examination of the SM predictions as well as potential NP sources of the discrepancies [1–4,16,18–21].

This Letter presents a measurement of direct CP asymmetry in the decay $B^+ \rightarrow K^+ \pi^0$,

$$A_{CP} = \frac{\Gamma(B^- \rightarrow K^-\pi^0) - \Gamma(B^+ \rightarrow K^+\pi^0)}{\Gamma(B^- \rightarrow K^-\pi^0) + \Gamma(B^+ \rightarrow K^+\pi^0)}, \quad (2)$$

where $\Gamma(B^\pm \rightarrow K^\pm \pi^0)$ refers to the rate of $B^\pm \rightarrow K^\pm \pi^0$ decays, using data recorded with the LHCb detector at the CERN Large Hadron Collider. The data sample corresponds to an integrated luminosity of 5.4 fb^{-1} collected at a center-of-mass energy of 13 TeV between 2016 and 2018.

The LHCb detector [23,24] is a single-arm forward spectrometer covering the pseudorapidity range $2 < \eta < 5$. The detector includes a high-precision tracking system consisting of a silicon-strip vertex detector surrounding the pp interaction region, a large-area silicon-strip detector located upstream of a dipole magnet with a bending power

*Full author list given at the end of the Letter.

Published by the American Physical Society under the terms of the Creative Commons Attribution 4.0 International license. Further distribution of this work must maintain attribution to the author(s) and the published article's title, journal citation, and DOI. Funded by SCOAP³.

of about 4 Tm, and three stations of silicon-strip detectors and straw drift tubes placed downstream of the magnet. The tracking system provides a measurement of momentum, p , of charged particles with a relative uncertainty that varies from 0.5% at low momentum to 1.0% at 200 GeV/c. The minimum distance of a track to a primary pp collision vertex (PV), the impact parameter (IP), is measured with a resolution of $(15 + 29/p_T) \mu\text{m}$, where p_T is the component of p transverse to the beam, in GeV/c. Different types of charged hadrons are distinguished using information from two ring-imaging Cherenkov detectors (RICH). Photons, electrons, and hadrons are identified by a calorimeter system consisting of scintillating pad and preshower detectors, an electromagnetic and a hadronic calorimeter. Charged and neutral clusters in the electromagnetic calorimeter (ECAL) are separated by extrapolating the tracks reconstructed by the tracking system to the calorimeter plane, while photons and neutral pions are distinguished by cluster shape and energy distributions.

Simulated events are used to model the effects of the detector acceptance and the imposed selection requirements. In the simulation, pp collisions are generated using PYTHIA [25] with a specific LHCb configuration [26]. Decays of unstable particles are described by EVTGEN [27], in which final-state radiation is generated using PHOTOS [28]. The interaction of the generated particles with the detector and its response are implemented using the GEANT4 toolkit [29], as described in Ref. [30].

The decay topology $B^+ \rightarrow h^+ \pi^0$, where h^+ is a charged hadron, presents a unique challenge in the proton-proton collision environment of the LHC. These decays comprise a single charged track and lack a reconstructible displaced vertex, a signature typically used to identify the decays of b hadrons. The candidate selection for $B^+ \rightarrow K^+ \pi^0$ candidates instead relies on identifying a charged kaon that is inconsistent with originating from any PV but consistent with originating from the B -meson trajectory. That trajectory is determined by adding the momenta of the K^+ and π^0 candidates, where the π^0 momentum is defined as pointing from the LHCb interaction point to the coordinate of the energy deposited by the π^0 candidate in the calorimeter.

The LHCb trigger system [31] consists of a hardware stage, based on information from the calorimeter and muon systems, followed by a software stage, in which a full event reconstruction is applied. Events are required to pass a hardware trigger that selects a neutral pion or photon with a high transverse energy based on energy deposits in the calorimeter. Because of the limited ECAL position resolution, a significant fraction of high $p_T \pi^0 \rightarrow \gamma\gamma$ decays have their photons merged into a single cluster. Only this π^0 category is used in this analysis, as neutral pions with the photons resolved suffer from a large background of randomly combined clusters. Further selection relies on a dedicated software trigger developed for this analysis [32]. A $B^+ \rightarrow K^+ \pi^0$ candidate is formed by adding the

four-momenta of the neutral pion and a charged track identified as a kaon using information from the RICH detectors. The charged kaon is required to have $p > 12 \text{ GeV}/c$, $p_T > 1.2 \text{ GeV}/c$, and a significant IP with respect to any PV. The neutral pion is required to have $p_T > 3.5 \text{ GeV}/c$ and the scalar sum of the K^+ and π^0 p_T must exceed $6.5 \text{ GeV}/c$. The B^+ candidate is required to have a $K^+ \pi^0$ invariant mass in the range $4 \leq m(K^+ \pi^0) \leq 6.2 \text{ GeV}/c^2$, and $p_T > 5 \text{ GeV}/c$. Finally, the B^+ candidate trajectory is obtained by fixing its momentum vector to the PV with the smallest kaon IP. The significance of the distance of closest approach between the K^+ candidate and this trajectory is denoted as DOCA- χ^2 . In order to identify K^+ candidates consistent with production via B -meson decay, the DOCA- χ^2 is required to be small. In the offline reconstruction, a stricter set of particle identification requirements are applied to the K^+ candidates.

Further candidate selection is based on variables characterizing how well isolated a candidate is from other tracks in the event. Vertex-isolation variables are calculated by combining each track in the event with the K^+ candidate individually to form a two-track secondary vertex. Three related variables are calculated: the smallest χ^2 of the vertex fit between the K^+ and any other track, the smallest change in χ^2 when one more track is added to that vertex, and the multiplicity of vertices having small χ^2 . The isolation of the candidate is also measured with the p_T asymmetry,

$$\mathcal{A}(p_T) = \frac{p_{T_B} - p_{T_{\text{cone}}}}{p_{T_B} + p_{T_{\text{cone}}}}, \quad (3)$$

comparing the transverse momentum of the B^+ candidate (p_{T_B}) to a scalar sum of additional charged particles nearby ($p_{T_{\text{cone}}}$). Particles are considered in a cone around the reconstructed B^+ trajectory with a radius in the η - ϕ plane of $\Delta R \equiv \sqrt{(\Delta\phi)^2 + (\Delta\eta)^2} = 1.7$, where $\Delta\phi$ is the difference in radians between the azimuthal angles of the momentum of the reconstructed B^+ candidate and the track, and $\Delta\eta$ is the difference between their pseudorapidities. To ensure that the simulated distributions of these variables for the signal decays are consistent with data, candidate weights are generated from the ratios of these distributions between simulated $B^0 \rightarrow K^+ \pi^-$ decays and a control sample of $B^0 \rightarrow K^+ \pi^-$ candidates selected in the same data set. A gradient boosted reweighter (GBR) [33] technique is used to determine the weights, which are subsequently applied to the $B^+ \rightarrow K^+ \pi^0$ simulations. The distribution of per-event weights applied to the $B^+ \rightarrow K^+ \pi^0$ simulation has a mean of 0.98 and a root mean square deviation of 0.28.

The final candidate selection is performed using boosted decision tree (BDT) classifiers with the isolation variables, the DOCA- χ^2 , the smallest change in χ^2 of the PV when including the K^+ track in the vertex fit, the p_T of the B^+

and the K^+ candidates, and the momentum of the π^0 candidate as inputs. These variables are chosen to provide discriminatory power between signal and background without biasing the $m(K^+\pi^0)$ distribution.

Two pairs of BDTs are trained and tested using data to represent background and simulated $B^+ \rightarrow K^+\pi^0$ decays, corrected as described above, to represent signal. One pair of BDTs is trained on background data with candidate invariant mass $m(K^+\pi^0) < 4860 \text{ MeV}/c^2$, which is dominated by partially reconstructed b -hadron decays. Another pair of BDTs is trained on background data with $m(K^+\pi^0) > 5700 \text{ MeV}/c^2$, which are primarily random $K^+\pi^0$ combinations (combinatorial background). In each of these categories, a cross-validation is performed. The data sample is split randomly, a BDT classifier is trained and tested on each half, and then used to assign a score to the candidates in the other half [34,35]. This avoids biases due to artifacts in the training samples, while taking advantage of the full set of data available. The optimal requirements on the two final classifier response variables are found for the data set simultaneously by maximizing ϵ/\sqrt{N} , where ϵ is the signal selection efficiency, evaluated on simulated events, and N is the total number of candidates observed in a region of approximately 3 times the observed $B^+ \rightarrow K^+\pi^0$ resolution around the expected B^+ mass.

Kaon candidates with $p_T > 17 \text{ GeV}/c$ or $p > 250 \text{ GeV}/c$ are removed from the sample after BDT selection because of insufficient coverage in the $B^+ \rightarrow J/\psi K^+$ control sample described below. They account for only 3% of the candidates after final selection.

The $m(K^+\pi^0)$ distribution of the selected $B^+ \rightarrow K^+\pi^0$ candidates, separated by the charge of the B meson, is shown in Fig. 1 along with the results of a fit to the data. In the fit, the signal is modeled by the sum of a Crystal Ball function [36] and a Gaussian function with an exponential tail describing the high-mass region. The Crystal Ball and the Gaussian functions share a common mean and width

that varies freely in the fit, and their tail shape parameters are fixed from simulation. Combinatorial background is modeled by an exponential function, with the exponent parameter allowed to vary freely in the fit. The tail of a Gaussian function is used to model the partially reconstructed background in the low-mass region, with mean and width allowed to vary freely in the fit. The rate of $\pi^+ \rightarrow K^+$ misidentification is measured in $D^0 \rightarrow K^-\pi^+$ decays as a function of pion momentum and pseudorapidity, with the same particle identification requirements as signal events [37]. The contribution of the misidentified $B^+ \rightarrow \pi^+\pi^0$ background is inferred from its branching fraction [38] and the misidentification rate to be 2.4% of the $B^+ \rightarrow K^+\pi^0$ yield. The $B^+ \rightarrow \pi^+\pi^0$ background component is modeled by a Gaussian with mean and resolution fixed to values determined from simulated events and a yield fixed to the expectation. There is assumed to be no asymmetry in this background.

An additional class of background candidates arises from decays such as $B^+ \rightarrow (K^{*+} \rightarrow K^+\pi^0)\pi^0$, $B^0 \rightarrow (K^{*0} \rightarrow K^+\pi^-)\pi^0$, and $B^0 \rightarrow K^+(\rho^- \rightarrow \pi^-\pi^0)$ where a pion from the K^* or ρ^- decay is not reconstructed. The polarization of the K^* or ρ^- meson results in a double peaked $m(K^+\pi^0)$ distribution, where the higher-mass peak is close to the expected B mass. This type of background is modeled with a parabolic function convolved with a Gaussian resolution function following the method described in Ref. [39]. The width of the resolution function is fixed to that of the signal resolution and the end points are fixed to the kinematic end points, allowing for a shift between the fitted and the known B^+ masses [38]. The lower-mass peak contributes below the $m(K^+\pi^0)$ range considered, and so its relative height is fixed to a value determined from simulation.

Other background sources include $B^+ \rightarrow (K^{*+} \rightarrow K^+\pi^0)\gamma$ decays where the γ is misidentified as a π^0 ; $B^+ \rightarrow (f^0(980) \rightarrow \pi^0\pi^0)K^+$ decays where one π^0 is not reconstructed; and $B^0 \rightarrow (\bar{D}^0 \rightarrow K^+\pi^-)\pi^0$,

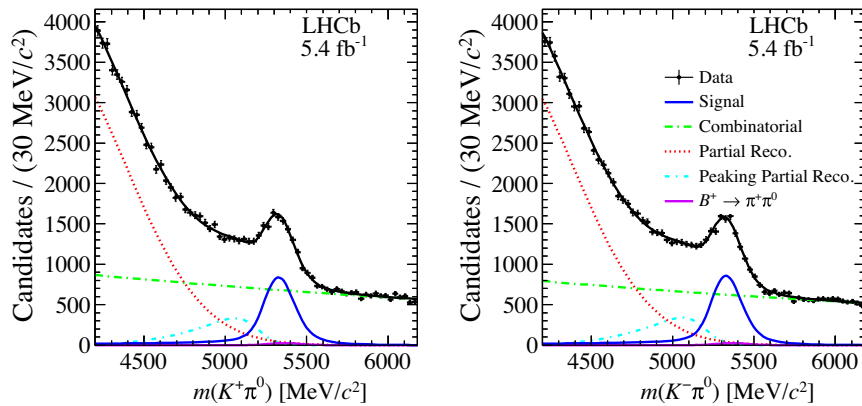


FIG. 1. Invariant-mass distribution of the selected candidates with fit projections overlaid. The data set is divided by the charge of the B meson, with $B^+ \rightarrow K^+\pi^0$ shown on the left and $B^- \rightarrow K^-\pi^0$ on the right.

$B^0 \rightarrow (K_0^*(1430) \rightarrow K^+\pi^-)\pi^0$, and $B_s^0 \rightarrow K^+\pi^0\pi^-$ decays where the π^- is not reconstructed. Simulation studies have shown that these background contributions either have $m(K^+\pi^0)$ distributions indistinguishable from the partially reconstructed samples described by a Gaussian tail, or in the case of $B_s^0 \rightarrow K^+\pi^0\pi^-$ has a branching fraction too small to give an observable contribution.

The data are fitted separately in four categories. In order to reduce uncertainties due to nonuniformity of the detector, candidates are separated according to whether the LHCb dipole magnetic field is aligned vertically upward (Magnet Up) or downward (Magnet Down) in the experiment. Candidates are further separated by B -meson charge in order to measure the CP asymmetry. The yield and asymmetry of each fit component are allowed to vary freely while the shape parameters are the same for the B^+ and B^- candidates. The total yield of $B^\pm \rightarrow K^\pm\pi^0$ decays is measured to be 8310 ± 255 in the Magnet Up data set and 8373 ± 253 in the Magnet Down data set. The raw asymmetry, A_{raw} , between the B^- and B^+ signal yields is found to be 0.019 ± 0.021 for Magnet Down and 0.005 ± 0.022 for Magnet Up. The results are consistent when candidates are separated by data-taking year as well as when shape parameters are allowed to vary independently for all four data categories.

As the measured asymmetry receives contributions from a number of nuisance asymmetries, the CP asymmetry can be expressed as

$$A_{CP}(B^+ \rightarrow K^+\pi^0) = A_{\text{raw}}(B^+ \rightarrow K^+\pi^0) - A_{\text{prod.}}^B - A_{\text{det.}}^K, \quad (4)$$

where $A_{\text{prod.}}^B$ is the production asymmetry of B^\pm mesons and $A_{\text{det.}}^K$ is the combined asymmetry in detection, triggering, and reconstruction of K^\pm mesons. These effects must be corrected for in order to extract A_{CP} from A_{raw} . The combined effect of the nuisance asymmetries is measured with a control sample of $B^+ \rightarrow (J/\psi \rightarrow \mu^+\mu^-)K^+$ decays, using the same data sample as the signal channel.

In the hardware trigger, events with a $B^+ \rightarrow (J/\psi \rightarrow \mu^+\mu^-)K^+$ decay are required to trigger on particles other than the kaon, in order to avoid introducing additional trigger asymmetries. At the software stage, the event must trigger on the kaon in the same manner as signal events. The offline selection requires that the B -meson decay time be greater than 0.1 ps and that the kaon and muons have a significant IP with respect to all PVs. Additional requirements on the momentum of the kaon and B candidates as well as kaon particle identification are imposed to match the signal selection. The momentum distributions of the B^+ and K^+ candidates are weighted to match those of the signal candidates using the GBR technique [33], as the production and detection asymmetries may depend on kinematics of the decay.

The raw asymmetry in the $B^+ \rightarrow J/\psi K^+$ signal yields is determined via an unbinned maximum-likelihood fit in which the invariant-mass distribution of the $B^+ \rightarrow J/\psi K^+$ candidates is modeled by the sum of two Gaussian functions sharing a common mean, while the combinatorial background is modeled by an exponential distribution. The total yield of $B^+ \rightarrow J/\psi K^+$ decays is measured to be 372874 ± 776 for Magnet Down and 306821 ± 699 for Magnet Up data samples with a purity of approximately 99%. The raw asymmetry is found to be -0.009 ± 0.002 for Magnet Up and -0.012 ± 0.002 for Magnet Down samples. The CP asymmetry for the decay $B^+ \rightarrow (J/\psi \rightarrow \mu^+\mu^-)K^+$ is taken to be $A_{CP}(B^+ \rightarrow J/\psi K^+) = 0.002 \pm 0.003$ from Ref. [38]. After subtracting A_{CP} , the remaining asymmetry is attributed to the combination of production, detection, reconstruction, and triggering effects, which can then be determined from

$$A_{\text{prod.}}^B + A_{\text{det.}}^K = A_{\text{raw}}(B^+ \rightarrow J/\psi K^+) - A_{CP}(B^+ \rightarrow J/\psi K^+). \quad (5)$$

This estimate of the nuisance asymmetry is then used in Eq. (4) to determine $A_{CP}(B^+ \rightarrow K^+\pi^0)$. This is done separately for the Magnet Up and Magnet Down data. By averaging the Magnet Up and Magnet Down results, the direct CP asymmetry is determined to be $A_{CP}(B^+ \rightarrow K^+\pi^0) = 0.025 \pm 0.015$, where the uncertainty is statistical only.

To assess the systematic uncertainty due to mismodeling of the signal and background line shapes, pseudoexperiments are generated for variations of the $m(K^+\pi^0)$ fit model. The leading source of systematic uncertainty is from modeling the signal component in the fit. This uncertainty is assessed by replacing the default model with a single Gaussian distribution. Systematic uncertainties are assessed for numerous fit variations: replacing the exponential distribution for the combinatorial background with a linear function, individually replacing each low-mass background model with an Argus function, allowing the position and resolution of the peaking low-mass background to vary freely and independently of the signal distribution, and varying the yield and asymmetry of $B^+ \rightarrow \pi^+\pi^0$ background. Pseudoexperiments are also generated to assess the systematic uncertainty due to including events with multiple candidates in the base analysis.

The statistical uncertainty on the determination of the raw $B^+ \rightarrow J/\psi K^+$ asymmetry is also considered as a systematic uncertainty and is the subdominant source of systematic uncertainty. Additionally, the difference between the nuisance asymmetries with and without applying the GBR weights is taken to be a systematic uncertainty. The estimated values for all systematic uncertainties are shown in Table I, where the common value of 0.0013 is from the statistical uncertainty of the pseudoexperiments generated.

TABLE I. Systematic uncertainties on $A_{CP}(B^+ \rightarrow K^+\pi^0)$.

Systematic	Value ($\times 10^{-3}$)
Signal modeling shape	4.3
Combinatorial background shape	1.3
Partial reco. background shape	1.3
Peaking partial reco. background shape	1.2
Peaking partial reco. background offset	1.3
Peaking partial reco. background resolution	1.4
$B^+ \rightarrow \pi^+\pi^0$ yield	1.3
$B^+ \rightarrow \pi^+\pi^0$ CP asymmetry	1.5
Multiple candidates	1.3
Production/detection asymmetry stat.	2.1
Production/detection asymmetry weights	0.5
Sum in quadrature	6.1

The $A_{CP}(B^+ \rightarrow J/\psi K^+)$ precision of 0.003 is considered separately as an external-input uncertainty.

In conclusion, the direct CP asymmetry of the decay $B^+ \rightarrow K^+\pi^0$ has been measured with the LHCb detector using a data sample corresponding to a luminosity of 5.4 fb^{-1} . It is found to be

$$A_{CP}(B^+ \rightarrow K^+\pi^0) = 0.025 \pm 0.015 \pm 0.006 \pm 0.003,$$

where the first uncertainty is statistical, the second is systematic, and the third due to external inputs, exceeding the precision of the current world average [22]. This result is consistent with the world average and consistent with zero at approximately 1.5σ . The CP asymmetry difference, $\Delta A_{CP}(K\pi) \equiv A_{CP}(B^+ \rightarrow K^+\pi^0) - A_{CP}(B^0 \rightarrow K^+\pi^-)$, is found to be 0.108 ± 0.017 , where $A_{CP}(B^0 \rightarrow K^+\pi^-)$ is taken from Ref. [22] (The world average includes the LHCb measurement, and a small correlation between the LHCb measurements of $A_{CP}(B^0 \rightarrow K^+\pi^-)$ and $A_{CP}(B^+ \rightarrow K^+\pi^0)$ due to the charged kaon detection asymmetry has been neglected.). Including the result presented in this Letter, the new world average of $A_{CP}(B^+ \rightarrow K^+\pi^0)$ is found to be 0.031 ± 0.013 . This corresponds to $\Delta A_{CP}(K\pi) = 0.115 \pm 0.014$, which is nonzero with a significance of more than 8 standard deviations, substantially enhanced over the results prior to this measurement. The updated sum rule prediction for $A_{CP}(B^0 \rightarrow K^0\pi^0)$, shown in Eq. (1), is found to be -0.138 ± 0.025 , departing from zero with a significance of approximately 5.5σ .

We express our gratitude to our colleagues in the CERN accelerator departments for the excellent performance of the LHC. We thank the technical and administrative staff at the LHCb institutes. We acknowledge support from CERN and from the national agencies: CAPES, CNPq, FAPERJ, and FINEP (Brazil); MOST and NSFC (China); CNRS/IN2P3 (France); BMBF, DFG, and MPG (Germany); INFN (Italy); NWO (Netherlands); MNiSW and NCN (Poland); MEN/IFA (Romania); MSHE (Russia); MICINN (Spain);

SNSF and SER (Switzerland); NASU (Ukraine); STFC (United Kingdom); DOE NP and NSF (USA). We acknowledge the computing resources that are provided by CERN, IN2P3 (France), KIT and DESY (Germany), INFN (Italy), SURF (Netherlands), PIC (Spain), GridPP (United Kingdom), RRCKI and Yandex LLC (Russia), CSCS (Switzerland), IFIN-HH (Romania), CBPF (Brazil), PL-GRID (Poland), and OSC (USA). We are indebted to the communities behind the multiple open-source software packages on which we depend. Individual groups or members have received support from AvH Foundation (Germany); EPLANET, Marie Skłodowska-Curie Actions, and ERC (European Union); A*MIDEX, ANR, Labex P2IO and OCEVU, and Région Auvergne-Rhône-Alpes (France); Key Research Program of Frontier Sciences of CAS, CAS PIFI, CAS CCEPP, Fundamental Research Funds for Central Universities, and Sci. and Tech. Program of Guangzhou (China); RFBR, RSF, and Yandex LLC (Russia); GVA, XuntaGal, and GENCAT (Spain); the Royal Society and the Leverhulme Trust (United Kingdom).

- [1] A. J. Buras, R. Fleischer, S. Recksiegel, and F. Schwab, The $B \rightarrow \pi K$ puzzle and its relation to rare B and K decays, *Eur. Phys. J. C* **32**, 45 (2003).
- [2] A. J. Buras, R. Fleischer, S. Recksiegel, and F. Schwab, $B \rightarrow \pi\pi$, New Physics in $B \rightarrow \pi K$, and Implications for Rare K and B Decays, *Phys. Rev. Lett.* **92**, 101804 (2004).
- [3] A. J. Buras, R. Fleischer, S. Recksiegel, and F. Schwab, Anatomy of prominent B and K decays and signatures of CP -violating new physics in the electroweak penguin sector, *Nucl. Phys.* **B697**, 133 (2004).
- [4] S. Baek *et al.*, $B \rightarrow \pi K$ puzzle and new physics, *Phys. Rev. D* **71**, 057502 (2005).
- [5] B. Aubert *et al.* (BABAR Collaboration), Direct CP Violating Asymmetry in $B^0 \rightarrow K^+\pi^-$ Decays, *Phys. Rev. Lett.* **93**, 131801 (2004).
- [6] Y. Chao *et al.* (Belle Collaboration), Evidence for Direct CP Violation in $B^0 \rightarrow K^+\pi^-$ Decays, *Phys. Rev. Lett.* **93**, 191802 (2004).
- [7] J. P. Lees (BABAR Collaboration), Measurement of CP asymmetries and branching fractions in charmless two-body B -meson decays to pions and kaons, *Phys. Rev. D* **87**, 052009 (2013).
- [8] Y.-T. Duh *et al.* (Belle Collaboration), Measurements of branching fractions and direct CP asymmetries for $B \rightarrow K\pi$, $B \rightarrow \pi\pi$ and $B \rightarrow KK$ decays, *Phys. Rev. D* **87**, 031103 (2013).
- [9] T. A. Aaltonen *et al.* (CDF Collaboration), Measurements of Direct CP -Violating Asymmetries in Charmless Decays of Bottom Baryons, *Phys. Rev. Lett.* **113**, 242001 (2014).
- [10] R. Aaij *et al.* (LHCb Collaboration), Measurement of CP asymmetries in two-body $B_{(s)}^0$ -meson decays to charged pions and kaons, *Phys. Rev. D* **98**, 032004 (2018).
- [11] B. Aubert *et al.* (BABAR Collaboration), Study of $B^0 \rightarrow \pi^0\pi^0$, $B^\pm \rightarrow \pi^\pm\pi^0$, and $B^\pm \rightarrow K^\pm\pi^0$ decays, and

- isospin analysis of $B \rightarrow \pi\pi$ decays, *Phys. Rev. D* **76**, 091102 (2007).
- [12] B. Aubert *et al.* (*BABAR* Collaboration), Measurement of time dependent CP asymmetry parameters in B^0 meson decays to ωK_S^0 , $\eta' K^0$, and $\pi^0 K_S^0$, *Phys. Rev. D* **79**, 052003 (2009).
- [13] M. Fujikawa *et al.* (*Belle* Collaboration), Measurement of CP asymmetries in $B^0 \rightarrow K^0\pi^0$ decays, *Phys. Rev. D* **81**, 011101 (2010).
- [14] B. Aubert *et al.* (*BABAR* Collaboration), Observation of $B^+ \rightarrow \bar{K}^0 K^+$ and $B^0 \rightarrow K^0 \bar{K}^0$, *Phys. Rev. Lett.* **97**, 171805 (2006).
- [15] R. Aaij *et al.* (*LHCb* Collaboration), Branching fraction and CP asymmetry of the decays $B^+ \rightarrow K_S^0 \pi^+$ and $B^+ \rightarrow K_S^0 K^+$, *Phys. Lett. B* **726**, 646 (2013).
- [16] S. Baek and D. London, Is there still a $B \rightarrow K\pi$ puzzle?, *Phys. Lett. B* **653**, 249 (2007).
- [17] M. Ciuchini *et al.*, Searching for new physics with $B \rightarrow K\pi$ decays, *Phys. Lett. B* **674**, 197 (2009).
- [18] S. Baek, C.-W. Chiang, and D. London, The $B \rightarrow K\pi$ puzzle: 2009 update, *Phys. Lett. B* **675**, 59 (2009).
- [19] M. Gronau, A precise sum rule among four $B \rightarrow K\pi CP$ asymmetries, *Phys. Lett. B* **627**, 82 (2005).
- [20] N. B. Beaudry *et al.*, The $B \rightarrow \pi K$ puzzle revisited, *J. High Energy Phys.* **01** (2018) 074.
- [21] R. Fleischer, R. Jaarsma, and K. K. Vos, Towards new frontiers with $B \rightarrow \pi K$ decays, *Phys. Lett. B* **785**, 525 (2018).
- [22] Y. Amhis *et al.* (Heavy Flavor Averaging Group), Averages of b -hadron, c -hadron, and τ -lepton properties as of 2018, updated results and plots available at <https://hflav.web.cern.ch>.
- [23] A. A. Alves Jr. *et al.* (*LHCb* Collaboration), The *LHCb* detector at the LHC, *J. Instrum.* **3**, S08005 (2008).
- [24] R. Aaij *et al.* (*LHCb* Collaboration), *LHCb* detector performance, *Int. J. Mod. Phys. A* **30**, 1530022 (2015).
- [25] T. Sjöstrand, S. Mrenna, and P. Skands, PYTHIA 6.4 physics and manual, *J. High Energy Phys.* **05** (2006) 026; T. Sjöstrand, S. Mrenna, and P. Skands, A brief introduction to PYTHIA 8.1, *Comput. Phys. Commun.* **178**, 852 (2008).
- [26] I. Belyaev *et al.*, Handling of the generation of primary events in Gauss, the *LHCb* simulation framework, *J. Phys. Conf. Ser.* **331**, 032047 (2011).
- [27] D. J. Lange, The *evtGen* particle decay simulation package, *Nucl. Instrum. Methods Phys. Res., Sect. A* **462**, 152 (2001).
- [28] P. Golonka and Z. Was, PHOTOS Monte Carlo: A precision tool for QED corrections in Z and W decays, *Eur. Phys. J. C* **45**, 97 (2006).
- [29] J. Allison *et al.* (*Geant4* Collaboration), GEANT4 developments and applications, *IEEE Trans. Nucl. Sci.* **53**, 270 (2006); S. Agostinelli *et al.* (*Geant4* Collaboration), GEANT4: A simulation toolkit, *Nucl. Instrum. Methods Phys. Res., Sect. A* **506**, 250 (2003).
- [30] M. Clemencic *et al.*, The *LHCb* simulation application, Gauss: Design, evolution and experience, *J. Phys. Conf. Ser.* **331**, 032023 (2011).
- [31] R. Aaij *et al.*, The *LHCb* trigger and its performance in 2011, *J. Instrum.* **8**, P04022 (2013).
- [32] *LHCb* Collaboration, Study of the decay $B^+ \rightarrow K^+\pi^0$ at *LHCb*, Report No. *LHCb-CONF-2015-001*, 2015, <https://cds.cern.ch/record/1988475>.
- [33] A. Rogozhnikov, Reweighting with boosted decision trees, *J. Phys. Conf. Ser.* **762**, 012036 (2016).
- [34] M. Stone, Cross-validatory choice and assessment of statistical predictions, *J. R. Stat. Soc. Ser. B (Methodological)* **36**, 111 (1974).
- [35] D. M. Allen, The relationship between variable selection and data augmentation and a method for prediction, *Technometrics* **16**, 125 (1974).
- [36] T. Skwarnicki, A study of the radiative cascade transitions between the Upsilon-prime and Upsilon resonances, Ph.D. thesis, Institute of Nuclear Physics, Krakow, 1986, DESY-F31-86-02, http://www-library.desy.de/preparch/desy/int_rep/f31-86-02.pdf.
- [37] L. Anderlini *et al.*, The PIDCalib package, *LHCb-PUB-2016-021*, 2016, <https://cds.cern.ch/record/2202412>.
- [38] P. A. Zyla *et al.* (Particle Data Group), Review of particle physics, *Prog. Theor. Exp. Phys.* **2020**, 083C01 (2020).
- [39] R. Aaij *et al.* (*LHCb* Collaboration), Measurement of CP observables in $B^\pm \rightarrow D K^\pm$ and $B^\pm \rightarrow D \pi^\pm$ with $D \rightarrow K_S^0 K^\pm \pi^\mp$ decays, *J. High Energy Phys.* **06** (2020) 58.

Correction: The first decay term appearing in the last sentence of the abstract contained an error and has been fixed.

R. Aaij,³² C. Abellán Beteta,⁵⁰ T. Ackernley,⁶⁰ B. Adeva,⁴⁶ M. Adinolfi,⁵⁴ H. Afsharnia,⁹ C. A. Aidala,⁸⁵ S. Aiola,²⁵ Z. Ajaltouni,⁹ S. Akar,⁶⁵ J. Albrecht,¹⁵ F. Alessio,⁴⁸ M. Alexander,⁵⁹ A. Alfonso Albero,⁴⁵ Z. Aliouche,⁶² G. Alkhazov,³⁸ P. Alvarez Cartelle,⁵⁵ S. Amato,² Y. Amhis,¹¹ L. An,⁴⁸ L. Anderlini,²² A. Andreianov,³⁸ M. Andreotti,²¹ J. E. Andrews,⁶⁶ F. Archilli,¹⁷ A. Artamonov,⁴⁴ M. Artuso,⁶⁸ K. Arzymatov,⁴² E. Aslanides,¹⁰ M. Atzeni,⁵⁰ B. Audurier,¹² S. Bachmann,¹⁷ M. Bachmayer,⁴⁹ J. J. Back,⁵⁶ S. Baker,⁶¹ P. Baladron Rodriguez,⁴⁶ V. Balagura,¹² W. Baldini,^{21,48} J. Baptista Leite,¹ R. J. Barlow,⁶² S. Barsuk,¹¹ W. Barter,⁶¹ M. Bartolini,^{24,a} F. Baryshnikov,⁸² J. M. Basels,¹⁴ G. Bassi,²⁹ B. Batsukh,⁶⁸ A. Battig,¹⁵ A. Bay,⁴⁹ M. Becker,¹⁵ F. Bedeschi,²⁹ I. Bediaga,¹ A. Beiter,⁶⁸ V. Belavin,⁴² S. Belin,²⁷ V. Bellee,⁴⁹ K. Belous,⁴⁴ I. Belov,⁴⁰ I. Belyaev,⁴¹ G. Bencivenni,²³ E. Ben-Haim,¹³ A. Berezhnoy,⁴⁰ R. Bernet,⁵⁰ D. Berninghoff,¹⁷ H. C. Bernstein,⁶⁸ C. Bertella,⁴⁸ E. Bertholet,¹³ A. Bertolin,²⁸ C. Betancourt,⁵⁰ F. Betti,^{20,b} Ia. Bezshyiko,⁵⁰ S. Bhasin,⁵⁴ J. Bhom,³⁵ L. Bian,⁷³ M. S. Bieker,¹⁵ S. Bifani,⁵³ P. Billoir,¹³ M. Birch,⁶¹ F. C. R. Bishop,⁵⁵ A. Bizzeti,^{22,c} M. Björn,⁶³ M. P. Blago,⁴⁸ T. Blake,⁵⁶ F. Blanc,⁴⁹ S. Blusk,⁶⁸ D. Bobulska,⁵⁹ J. A. Boelhauve,¹⁵ O. Boente Garcia,⁴⁶ T. Boettcher,⁶⁴ A. Boldyrev,⁸¹ A. Bondar,⁴³

- N. Bondar,^{38,48} S. Borghi,⁶² M. Borisyak,⁴² M. Borsato,¹⁷ J. T. Borsuk,³⁵ S. A. Bouchiba,⁴⁹ T. J. V. Bowcock,⁶⁰ A. Boyer,⁴⁸ C. Bozzi,²¹ M. J. Bradley,⁶¹ S. Braun,⁶⁶ A. Brea Rodriguez,⁴⁶ M. Brodski,⁴⁸ J. Brodzicka,³⁵ A. Brossa Gonzalo,⁵⁶ D. Brundu,²⁷ A. Buonaura,⁵⁰ C. Burr,⁴⁸ A. Bursche,²⁷ A. Butkevich,³⁹ J. S. Butter,³² J. Buytaert,⁴⁸ W. Byczynski,⁴⁸ S. Cadeddu,²⁷ H. Cai,⁷³ R. Calabrese,^{21,d} L. Calefice,^{15,13} L. Calero Diaz,²³ S. Cali,²³ R. Calladine,⁵³ M. Calvi,^{26,e} M. Calvo Gomez,⁸⁴ P. Camargo Magalhaes,⁵⁴ A. Camboni,^{45,84} P. Campana,²³ A. F. Campoverde Quezada,⁶ S. Capelli,^{26,e} L. Capriotti,^{20,b} A. Carbone,^{20,b} G. Carboni,³¹ R. Cardinale,^{24,a} A. Cardini,²⁷ I. Carli,⁴ P. Carniti,^{26,e} L. Carus,¹⁴ K. Carvalho Akiba,³² A. Casais Vidal,⁴⁶ G. Casse,⁶⁰ M. Cattaneo,⁴⁸ G. Cavallero,⁴⁸ S. Celani,⁴⁹ J. Cerasoli,¹⁰ A. J. Chadwick,⁶⁰ M. G. Chapman,⁵⁴ M. Charles,¹³ Ph. Charpentier,⁴⁸ G. Chatzikonstantinidis,⁵³ C. A. Chavez Barajas,⁶⁰ M. Chefdeville,⁸ C. Chen,³ S. Chen,²⁷ A. Chernov,³⁵ S.-G. Chitic,⁴⁸ V. Chobanova,⁴⁶ S. Cholak,⁴⁹ M. Chrzaszcz,³⁵ A. Chubykin,³⁸ V. Chulikov,³⁸ P. Ciambrone,²³ M. F. Cicala,⁵⁶ X. Cid Vidal,⁴⁶ G. Ciezarek,⁴⁸ P. E. L. Clarke,⁵⁸ M. Clemencic,⁴⁸ H. V. Cliff,⁵⁵ J. Closier,⁴⁸ J. L. Cobbledick,⁶² V. Coco,⁴⁸ J. A. B. Coelho,¹¹ J. Cogan,¹⁰ E. Cogneras,⁹ L. Cojocariu,³⁷ P. Collins,⁴⁸ T. Colombo,⁴⁸ L. Congedo,^{19,f} A. Contu,²⁷ N. Cooke,⁵³ G. Coombs,⁵⁹ G. Corti,⁴⁸ C. M. Costa Sobral,⁵⁶ B. Couturier,⁴⁸ D. C. Craik,⁶⁴ J. Crkovská,⁶⁷ M. Cruz Torres,¹ R. Currie,⁵⁸ C. L. Da Silva,⁶⁷ E. Dall'Occo,¹⁵ J. Dalseno,⁴⁶ C. D'Ambrosio,⁴⁸ A. Danilina,⁴¹ P. d'Argent,⁴⁸ A. Davis,⁶² O. De Aguiar Francisco,⁶² K. De Bruyn,⁷⁸ S. De Capua,⁶² M. De Cian,⁴⁹ J. M. De Miranda,¹ L. De Paula,² M. De Serio,^{19,f} D. De Simone,⁵⁰ P. De Simone,²³ J. A. de Vries,⁷⁹ C. T. Dean,⁶⁷ W. Dean,⁸⁵ D. Decamp,⁸ L. Del Buono,¹³ B. Delaney,⁵⁵ H.-P. Dembinski,¹⁵ A. Dendek,³⁴ V. Denysenko,⁵⁰ D. Derkach,⁸¹ O. Deschamps,⁹ F. Desse,¹¹ F. Dettori,^{27,g} B. Dey,⁷³ P. Di Nezza,²³ S. Didenko,⁸² L. Dieste Maronas,⁴⁶ H. Dijkstra,⁴⁸ V. Dobishuk,⁵² A. M. Donohoe,¹⁸ F. Dordei,²⁷ A. C. dos Reis,¹ L. Douglas,⁵⁹ A. Dovbnya,⁵¹ A. G. Downes,⁸ K. Dreimanis,⁶⁰ M. W. Dudek,³⁵ L. Dufour,⁴⁸ V. Duk,⁷⁷ P. Durante,⁴⁸ J. M. Durham,⁶⁷ D. Dutta,⁶² M. Dziewiecki,¹⁷ A. Dziurda,³⁵ A. Dzyuba,³⁸ S. Easo,⁵⁷ U. Egede,⁶⁹ V. Egorychev,⁴¹ S. Eidelman,^{43,h} S. Eisenhardt,⁵⁸ S. Ek-In,⁴⁹ L. Eklund,⁵⁹ S. Ely,⁶⁸ A. Ene,³⁷ E. Epple,⁶⁷ S. Escher,¹⁴ J. Eschle,⁵⁰ S. Esen,³² T. Evans,⁴⁸ A. Falabella,²⁰ J. Fan,³ Y. Fan,⁶ B. Fang,⁷³ N. Farley,⁵³ S. Farry,⁶⁰ D. Fazzini,^{26,e} P. Fedin,⁴¹ M. Féo,⁴⁸ P. Fernandez Declara,⁴⁸ A. Fernandez Prieto,⁴⁶ J. M. Fernandez-tenllado Arribas,⁴⁵ F. Ferrari,^{20,b} L. Ferreira Lopes,⁴⁹ F. Ferreira Rodrigues,² S. Ferreres Sole,³² M. Ferrillo,⁵⁰ M. Ferro-Luzzi,⁴⁸ S. Filippov,³⁹ R. A. Fini,¹⁹ M. Fiorini,^{21,d} M. Firlej,³⁴ K. M. Fischer,⁶³ C. Fitzpatrick,⁶² T. Fiutowski,³⁴ F. Fleuret,¹² M. Fontana,¹³ F. Fontanelli,^{24,a} R. Forty,⁴⁸ V. Franco Lima,⁶⁰ M. Franco Sevilla,⁶⁶ M. Frank,⁴⁸ E. Franzoso,²¹ G. Frau,¹⁷ C. Frei,⁴⁸ D. A. Friday,⁵⁹ J. Fu,²⁵ Q. Fuehring,¹⁵ W. Funk,⁴⁸ E. Gabriel,³² T. Gaintseva,⁴² A. Gallas Torreira,⁴⁶ D. Galli,^{20,b} S. Gambetta,^{58,48} Y. Gan,³ M. Gandelman,² P. Gandini,²⁵ Y. Gao,⁵ M. Garau,²⁷ L. M. Garcia Martin,⁵⁶ P. Garcia Moreno,⁴⁵ J. García Pardiñas,²⁶ B. Garcia Plana,⁴⁶ F. A. Garcia Rosales,¹² L. Garrido,⁴⁵ C. Gaspar,⁴⁸ R. E. Geertsema,³² D. Gerick,¹⁷ L. L. Gerken,¹⁵ E. Gersabeck,⁶² M. Gersabeck,⁶² T. Gershon,⁵⁶ D. Gerstel,¹⁰ Ph. Ghez,⁸ V. Gibson,⁵⁵ M. Giovannetti,^{23,i} A. Gioventù,⁴⁶ P. Gironella Gironell,⁴⁵ L. Giubega,³⁷ C. Giugliano,^{21,48,d} K. Gizdov,⁵⁸ E. L. Gkougkousis,⁴⁸ V. V. Gligorov,¹³ C. Göbel,⁷⁰ E. Golobardes,⁸⁴ D. Golubkov,⁴¹ A. Golutvin,^{61,82} A. Gomes,^{1,j} S. Gomez Fernandez,⁴⁵ F. Goncalves Abrantes,⁷⁰ M. Goncerz,³⁵ G. Gong,³ P. Gorbounov,⁴¹ I. V. Gorelov,⁴⁰ C. Gotti,²⁶ E. Govorkova,⁴⁸ J. P. Grabowski,¹⁷ R. Graciani Diaz,⁴⁵ T. Grammatico,¹³ L. A. Granado Cardoso,⁴⁸ E. Graugés,⁴⁵ E. Graverini,⁴⁹ G. Graziani,²² A. Grecu,³⁷ L. M. Greeven,³² P. Griffith,^{21,d} L. Grillo,⁶² S. Gromov,⁸² B. R. Gruberg Cazon,⁶³ C. Gu,³ M. Guarise,²¹ P. A. Günther,¹⁷ E. Gushchin,³⁹ A. Guth,¹⁴ Y. Guz,^{44,48} T. Gys,⁴⁸ T. Hadavizadeh,⁶⁹ G. Haefeli,⁴⁹ C. Haen,⁴⁸ J. Haimberger,⁴⁸ T. Halewood-leagas,⁶⁰ P. M. Hamilton,⁶⁶ Q. Han,⁷ X. Han,¹⁷ T. H. Hancock,⁶³ S. Hansmann-Menzemer,¹⁷ N. Harnew,⁶³ T. Harrison,⁶⁰ C. Hasse,⁴⁸ M. Hatch,⁴⁸ J. He,⁶ M. Hecker,⁶¹ K. Heijhoff,³² K. Heinicke,¹⁵ A. M. Hennequin,⁴⁸ K. Hennessy,⁶⁰ L. Henry,^{25,47} J. Heuel,¹⁴ A. Hicheur,² D. Hill,⁴⁹ M. Hilton,⁶² S. E. Hollitt,¹⁵ J. Hu,¹⁷ J. Hu,⁷² W. Hu,⁷ W. Huang,⁶ X. Huang,⁷³ W. Hulsbergen,³² R. J. Hunter,⁵⁶ M. Hushchyn,⁸¹ D. Hutchcroft,⁶⁰ D. Hynds,³² P. Ibis,¹⁵ M. Idzik,³⁴ D. Ilin,³⁸ P. Ilten,⁶⁵ A. Inglessi,³⁸ A. Ishteev,⁸² K. Ivshin,³⁸ R. Jacobsson,⁴⁸ S. Jakobsen,⁴⁸ E. Jans,³² B. K. Jashal,⁴⁷ A. Jawahery,⁶⁶ V. Jevtic,¹⁵ M. Jezabek,³⁵ F. Jiang,³ M. John,⁶³ D. Johnson,⁴⁸ C. R. Jones,⁵⁵ T. P. Jones,⁵⁶ B. Jost,⁴⁸ N. Jurik,⁴⁸ S. Kandybei,⁵¹ Y. Kang,³ M. Karacson,⁴⁸ M. Karpov,⁸¹ N. Kazeev,⁸¹ F. Keizer,^{55,48} M. Kenzie,⁵⁶ T. Ketel,³³ B. Khanji,¹⁵ A. Kharisova,⁸³ S. Kholodenko,⁴⁴ K. E. Kim,⁶⁸ T. Kirn,¹⁴ V. S. Kirsebom,⁴⁹ O. Kitouni,⁶⁴ S. Klaver,³² K. Klimaszewski,³⁶ S. Koliev,⁵² A. Kondybayeva,⁸² A. Konoplyannikov,⁴¹ P. Kopciewicz,³⁴ R. Kopecna,¹⁷ P. Koppenburg,³² M. Korolev,⁴⁰ I. Kostiuk,^{32,52} O. Kot,⁵² S. Kotriakhova,^{38,30} P. Kravchenko,³⁸ L. Kravchuk,³⁹ R. D. Krawczyk,⁴⁸ M. Kreps,⁵⁶ F. Kress,⁶¹ S. Kretschmar,¹⁴ P. Krokovny,^{43,h} W. Krupa,³⁴ W. Krzemien,³⁶ W. Kucewicz,^{35,k} M. Kucharczyk,³⁵ V. Kudryavtsev,^{43,h} H. S. Kuindersma,³² G. J. Kunde,⁶⁷ T. Kvaratskheliya,⁴¹ D. Lacarrere,⁴⁸ G. Lafferty,⁶² A. Lai,²⁷ A. Lampis,²⁷ D. Lancierini,⁵⁰ J. J. Lane,⁶² R. Lane,⁵⁴ G. Lanfranchi,²³ C. Langenbruch,¹⁴ J. Langer,¹⁵ O. Lantwin,^{50,82} T. Latham,⁵⁶ F. Lazzari,^{29,l} R. Le Gac,¹⁰

- S. H. Lee,⁸⁵ R. Lefèvre,⁹ A. Leflat,⁴⁰ S. Legotin,⁸² O. Leroy,¹⁰ T. Lesiak,³⁵ B. Leverington,¹⁷ H. Li,⁷² L. Li,⁶³ P. Li,¹⁷ Y. Li,⁴ Y. Li,⁴ Z. Li,⁶⁸ X. Liang,⁶⁸ T. Lin,⁶¹ R. Lindner,⁴⁸ V. Lisovskyi,¹⁵ R. Litvinov,²⁷ G. Liu,⁷² H. Liu,⁶ S. Liu,⁴ X. Liu,³ A. Loi,²⁷ J. Lomba Castro,⁴⁶ I. Longstaff,⁵⁹ J. H. Lopes,² G. Loustau,⁵⁰ G. H. Lovell,⁵⁵ Y. Lu,⁴ D. Lucchesi,^{28,m} S. Luchuk,³⁹ M. Lucio Martinez,³² V. Lukashenko,³² Y. Luo,³ A. Lupato,⁶² E. Luppi,^{21,d} O. Lupton,⁵⁶ A. Lusiani,^{29,n} X. Lyu,⁶ L. Ma,⁴ R. Ma,⁶ S. Maccolini,^{20,b} F. Machefert,¹¹ F. Maciuc,³⁷ V. Macko,⁴⁹ P. Mackowiak,¹⁵ S. Maddrell-Mander,⁵⁴ O. Madejczyk,³⁴ L. R. Madhan Mohan,⁵⁴ O. Maev,³⁸ A. Maevskiy,⁸¹ D. Maisuzenko,³⁸ M. W. Majewski,³⁴ J. J. Malczewski,³⁵ S. Malde,⁶³ B. Malecki,⁴⁸ A. Malinin,⁸⁰ T. Maltsev,^{43,h} H. Malygina,¹⁷ G. Manca,^{27,g} G. Mancinelli,¹⁰ R. Manera Escalero,⁴⁵ D. Manuzzi,^{20,b} D. Marangotto,^{25,o} J. Maratas,^{9,p} J. F. Marchand,⁸ U. Marconi,²⁰ S. Mariami,^{22,48,q} C. Marin Benito,¹¹ M. Marinangeli,⁴⁹ P. Marino,^{49,n} J. Marks,¹⁷ P. J. Marshall,⁶⁰ G. Martellotti,³⁰ L. Martinazzoli,^{48,e} M. Martinelli,^{26,e} D. Martinez Santos,⁴⁶ F. Martinez Vidal,⁴⁷ A. Massafferri,¹ M. Materok,¹⁴ R. Matev,⁴⁸ A. Mathad,⁵⁰ Z. Mathe,⁴⁸ V. Matiunin,⁴¹ C. Matteuzzi,²⁶ K. R. Mattioli,⁸⁵ A. Mauri,³² E. Maurice,¹² J. Mauricio,⁴⁵ M. Mazurek,³⁶ M. McCann,⁶¹ L. Mcconnell,¹⁸ T. H. McGrath,⁶² A. McNab,⁶² R. McNulty,¹⁸ J. V. Mead,⁶⁰ B. Meadows,⁶⁵ C. Meaux,¹⁰ G. Meier,¹⁵ N. Meinert,⁷⁶ D. Melnychuk,³⁶ S. Meloni,^{26,e} M. Merk,^{32,79} A. Merli,²⁵ L. Meyer Garcia,² M. Mikhasenko,⁴⁸ D. A. Milanes,⁷⁴ E. Millard,⁵⁶ M. Milovanovic,⁴⁸ M.-N. Minard,⁸ L. Minzoni,^{21,d} S. E. Mitchell,⁵⁸ B. Mitreska,⁶² D. S. Mitzel,⁴⁸ A. Mödden,¹⁵ R. A. Mohammed,⁶³ R. D. Moise,⁶¹ T. Mombächer,¹⁵ I. A. Monroy,⁷⁴ S. Monteil,⁹ M. Morandin,²⁸ G. Morello,²³ M. J. Morello,^{29,n} J. Moron,³⁴ A. B. Morris,⁷⁵ A. G. Morris,⁵⁶ R. Mountain,⁶⁸ H. Mu,³ F. Muheim,⁵⁸ M. Mukherjee,⁷ M. Mulder,⁴⁸ D. Müller,⁴⁸ K. Müller,⁵⁰ C. H. Murphy,⁶³ D. Murray,⁶² P. Muzzetto,^{27,48} P. Naik,⁵⁴ T. Nakada,⁴⁹ R. Nandakumar,⁵⁷ T. Nanut,⁴⁹ I. Nasteva,² M. Needham,⁵⁸ I. Neri,^{21,d} N. Neri,^{25,o} S. Neubert,⁷⁵ N. Neufeld,⁴⁸ R. Newcombe,⁶¹ T. D. Nguyen,^{49,r} C. Nguyen-Mau,^{49,r} E. M. Niel,¹¹ S. Nieswand,¹⁴ N. Nikitin,⁴⁰ N. S. Nolte,⁴⁸ C. Nunez,⁸⁵ A. Oblakowska-Mucha,³⁴ V. Obraztsov,⁴⁴ D. P. O'Hanlon,⁵⁴ R. Oldeman,^{27,g} M. E. Olivares,⁶⁸ C. J. G. Onderwater,⁷⁸ A. Ossowska,³⁵ J. M. Otalora Goicochea,² T. Ovsiannikova,⁴¹ P. Owen,⁵⁰ A. Oyanguren,⁴⁷ B. Pagare,⁵⁶ P. R. Pais,⁴⁸ T. Pajero,^{29,48,n} A. Palano,¹⁹ M. Palutan,²³ Y. Pan,⁶² G. Panshin,⁸³ A. Papanestis,⁵⁷ M. Pappagallo,^{19,f} L. L. Pappalardo,^{21,d} C. Pappenheimer,⁶⁵ W. Parker,⁶⁶ C. Parkes,⁶² C. J. Parkinson,⁴⁶ B. Passalacqua,²¹ G. Passaleva,²² A. Pastore,¹⁹ M. Patel,⁶¹ C. Patrignani,^{20,b} C. J. Pawley,⁷⁹ A. Pearce,⁴⁸ A. Pellegrino,³² M. Pepe Altarelli,⁴⁸ S. Perazzini,²⁰ D. Pereima,⁴¹ P. Perret,⁹ K. Petridis,⁵⁴ A. Petrolini,^{24,a} A. Petrov,⁸⁰ S. Petrucci,⁵⁸ M. Petruzzo,²⁵ T. T. H. Pham,⁶⁸ A. Philippov,⁴² L. Pica,²⁹ M. Piccini,⁷⁷ B. Pietrzyk,⁸ G. Pietrzyk,⁴⁹ M. Pili,⁶³ D. Pinci,³⁰ F. Pisani,⁴⁸ A. Piucci,¹⁷ Resmi P. K.,¹⁰ V. Placinta,³⁷ J. Plews,⁵³ M. Plo Casasus,⁴⁶ F. Polci,¹³ M. Poli Lener,²³ M. Poliakova,⁶⁸ A. Poluektov,¹⁰ N. Polukhina,^{82,s} I. Polyakov,⁶⁸ E. Polycarpo,² G. J. Pomery,⁵⁴ S. Ponce,⁴⁸ D. Popov,^{6,48} S. Popov,⁴² S. Poslavskii,⁴⁴ K. Prasanth,³⁵ L. Promberger,⁴⁸ C. Prouve,⁴⁶ V. Pugatch,⁵² H. Pullen,⁶³ G. Punzi,^{29,t} W. Qian,⁶ J. Qin,⁶ R. Quagliani,¹³ B. Quintana,⁸ N. V. Raab,¹⁸ R. I. Rabadan Trejo,¹⁰ B. Rachwal,³⁴ J. H. Rademacker,⁵⁴ M. Rama,²⁹ M. Ramos Pernas,⁵⁶ M. S. Rangel,² F. Ratnikov,^{42,81} G. Raven,³³ M. Reboud,⁸ F. Redi,⁴⁹ F. Reiss,¹³ C. Remon Alepuz,⁴⁷ Z. Ren,³ V. Renaudin,⁶³ R. Ribatti,²⁹ S. Ricciardi,⁵⁷ K. Rinnert,⁶⁰ P. Robbe,¹¹ A. Robert,¹³ G. Robertson,⁵⁸ A. B. Rodrigues,⁴⁹ E. Rodrigues,⁶⁰ J. A. Rodriguez Lopez,⁷⁴ A. Rollings,⁶³ P. Roloff,⁴⁸ V. Romanovskiy,⁴⁴ M. Romero Lamas,⁴⁶ A. Romero Vidal,⁴⁶ J. D. Roth,⁸⁵ M. Rotondo,²³ M. S. Rudolph,⁶⁸ T. Ruf,⁴⁸ J. Ruiz Vidal,⁴⁷ A. Ryzhikov,⁸¹ J. Ryzka,³⁴ J. J. Saborido Silva,⁴⁶ N. Sagidova,³⁸ N. Sahoo,⁵⁶ B. Saitta,^{27,g} D. Sanchez Gonzalo,⁴⁵ C. Sanchez Gras,³² R. Santacesaria,³⁰ C. Santamarina Rios,⁴⁶ M. Santimaria,²³ E. Santovetti,^{31,i} D. Saranin,⁸² G. Sarpis,⁵⁹ M. Sarpis,⁷⁵ A. Sarti,³⁰ C. Satriano,^{30,u} A. Satta,³¹ M. Saur,¹⁵ D. Savrina,^{41,40} H. Sazak,⁹ L. G. Scantlebury Smead,⁶³ S. Schael,¹⁴ M. Schellenberg,¹⁵ M. Schiller,⁵⁹ H. Schindler,⁴⁸ M. Schmelling,¹⁶ B. Schmidt,⁴⁸ O. Schneider,⁴⁹ A. Schopper,⁴⁸ M. Schubiger,³² S. Schulte,⁴⁹ M. H. Schune,¹¹ R. Schwemmer,⁴⁸ B. Sciascia,²³ A. Sciubba,²³ S. Sellam,⁴⁶ A. Semennikov,⁴¹ M. Senghi Soares,³³ A. Sergi,^{53,48} N. Serra,⁵⁰ L. Sestini,²⁸ A. Seuthe,¹⁵ P. Seyfert,⁴⁸ D. M. Shangase,⁸⁵ M. Shapkin,⁴⁴ I. Shchemerov,⁸² L. Shchutska,⁴⁹ T. Shears,⁶⁰ L. Shekhtman,^{43,h} Z. Shen,⁵ V. Shevchenko,⁸⁰ E. B. Shields,^{26,e} E. Shmanin,⁸² J. D. Shupperd,⁶⁸ B. G. Siddi,²¹ R. Silva Coutinho,⁵⁰ G. Simi,²⁸ S. Simone,^{19,f} I. Skiba,^{21,d} N. Skidmore,⁶² T. Skwarnicki,⁶⁸ M. W. Slater,⁵³ J. C. Smallwood,⁶³ J. G. Smeaton,⁵⁵ A. Smetkina,⁴¹ E. Smith,¹⁴ M. Smith,⁶¹ A. Snoch,³² M. Soares,²⁰ L. Soares Lavra,⁹ M. D. Sokoloff,⁶⁵ F. J. P. Soler,⁵⁹ A. Solovev,³⁸ I. Solovyev,³⁸ F. L. Souza De Almeida,² B. Souza De Paula,² B. Spaan,¹⁵ E. Spadaro Norella,^{25,o} P. Spradlin,⁵⁹ F. Stagni,⁴⁸ M. Stahl,⁶⁵ S. Stahl,⁴⁸ P. Steffko,⁴⁹ O. Steinkamp,^{50,82} S. Stemmle,¹⁷ O. Stenyakin,⁴⁴ H. Stevens,¹⁵ S. Stone,⁶⁸ M. E. Stramaglia,⁴⁹ M. Straticiuc,³⁷ D. Strekalina,⁸² S. Strokov,⁸³ F. Suljik,⁶³ J. Sun,²⁷ L. Sun,⁷³ Y. Sun,⁶⁶ P. Svihra,⁶² P. N. Swallow,⁵³ K. Swientek,³⁴ A. Szabelski,³⁶ T. Szumlak,³⁴ M. Szymanski,⁴⁸ S. Taneja,⁶² F. Teubert,⁴⁸ E. Thomas,⁴⁸ K. A. Thomson,⁶⁰ M. J. Tilley,⁶¹ V. Tisserand,⁹ S. T'Jampens,⁸ M. Tobin,⁴ S. Tolk,⁴⁸ L. Tomassetti,^{21,d} D. Torres Machado,¹ D. Y. Tou,¹³ M. Traill,⁵⁹

M. T. Tran,⁴⁹ E. Trifonova,⁸² C. Tripli,⁴⁹ G. Tuci,^{29,b} A. Tully,⁴⁹ N. Tuning,³² A. Ukleja,³⁶ D. J. Unverzagt,¹⁷ E. Ursov,⁸² A. Usachov,³² A. Ustyuzhanin,^{42,81} U. Uwer,¹⁷ A. Wagner,⁸³ V. Vagnoni,²⁰ A. Valassi,⁴⁸ G. Valenti,²⁰ N. Valls Canudas,⁴⁵ M. van Beuzekom,³² M. Van Dijk,⁴⁹ E. van Herwijnen,⁸² C. B. Van Hulse,¹⁸ M. van Veghel,⁷⁸ R. Vazquez Gomez,⁴⁶ P. Vazquez Regueiro,⁴⁶ C. Vázquez Sierra,⁴⁸ S. Vecchi,²¹ J. J. Velthuis,⁵⁴ M. Veltri,^{22,b} A. Venkateswaran,⁶⁸ M. Veronesi,³² M. Vesterinen,⁵⁶ D. Vieira,⁶⁵ M. Vieites Diaz,⁴⁹ H. Viemann,⁷⁶ X. Vilasis-Cardona,⁸⁴ E. Vilella Figueiras,⁶⁰ P. Vincent,¹³ G. Vitali,²⁹ A. Vollhardt,⁵⁰ D. Vom Bruch,¹³ A. Vorobyev,³⁸ V. Vorobyev,^{43,b} N. Voropaev,³⁸ R. Waldi,⁷⁶ J. Walsh,²⁹ C. Wang,¹⁷ J. Wang,⁵ J. Wang,⁴ J. Wang,³ J. Wang,⁷³ M. Wang,³ R. Wang,⁵⁴ Y. Wang,⁷ Z. Wang,⁵⁰ H. M. Wark,⁶⁰ N. K. Watson,⁵³ S. G. Weber,¹³ D. Websdale,⁶¹ C. Weisser,⁶⁴ B. D. C. Westhenry,⁵⁴ D. J. White,⁶² M. Whitehead,⁵⁴ D. Wiedner,¹⁵ G. Wilkinson,⁶³ M. Wilkinson,⁶⁸ I. Williams,⁵⁵ M. Williams,^{64,69} M. R. J. Williams,⁵⁸ F. F. Wilson,⁵⁷ W. Wislicki,³⁶ M. Witek,³⁵ L. Witola,¹⁷ G. Wormser,¹¹ S. A. Wotton,⁵⁵ H. Wu,⁶⁸ K. Wyllie,⁴⁸ Z. Xiang,⁶ D. Xiao,⁷ Y. Xie,⁷ A. Xu,⁵ J. Xu,⁶ L. Xu,³ M. Xu,⁷ Q. Xu,⁶ Z. Xu,⁵ Z. Xu,⁶ D. Yang,³ S. Yang,⁶ Y. Yang,⁶ Z. Yang,³ Z. Yang,⁶⁶ Y. Yao,⁶⁸ L. E. Yeomans,⁶⁰ H. Yin,⁷ J. Yu,⁷¹ X. Yuan,⁶⁸ O. Yushchenko,⁴⁴ E. Zaffaroni,⁴⁹ K. A. Zarebski,⁵³ M. Zavertyaev,^{16,s} M. Zdybal,³⁵ O. Zenayev,⁴⁸ M. Zeng,³ D. Zhang,⁷ L. Zhang,³ S. Zhang,⁵ Y. Zhang,⁵ Y. Zhang,⁶³ A. Zhelezov,¹⁷ Y. Zheng,⁶ X. Zhou,⁶ Y. Zhou,⁶ X. Zhu,³ V. Zhukov,^{14,40} J. B. Zonneveld,⁵⁸ S. Zucchelli,^{20,b} D. Zuliani,²⁸ and G. Zunică⁶²

(LHCb Collaboration)

¹*Centro Brasileiro de Pesquisas Físicas (CBPF), Rio de Janeiro, Brazil*²*Universidade Federal do Rio de Janeiro (UFRJ), Rio de Janeiro, Brazil*³*Center for High Energy Physics, Tsinghua University, Beijing, China*⁴*Institute Of High Energy Physics (IHEP), Beijing, China*⁵*School of Physics State Key Laboratory of Nuclear Physics and Technology, Peking University, Beijing, China*⁶*University of Chinese Academy of Sciences, Beijing, China*⁷*Institute of Particle Physics, Central China Normal University, Wuhan, Hubei, China*⁸*Univ. Grenoble Alpes, Univ. Savoie Mont Blanc, CNRS, IN2P3-LAPP, Annecy, France*⁹*Université Clermont Auvergne, CNRS/IN2P3, LPC, Clermont-Ferrand, France*¹⁰*Aix Marseille Univ, CNRS/IN2P3, CPPM, Marseille, France*¹¹*Université Paris-Saclay, CNRS/IN2P3, IJCLab, Orsay, France*¹²*Laboratoire Leprince-ringuet (llr), Palaiseau, France*¹³*LPNHE, Sorbonne Université, Paris Diderot Sorbonne Paris Cité, CNRS/IN2P3, Paris, France*¹⁴*I. Physikalisches Institut, RWTH Aachen University, Aachen, Germany*¹⁵*Fakultät Physik, Technische Universität Dortmund, Dortmund, Germany*¹⁶*Max-Planck-Institut für Kernphysik (MPIK), Heidelberg, Germany*¹⁷*Physikalisches Institut, Ruprecht-Karls-Universität Heidelberg, Heidelberg, Germany*¹⁸*School of Physics, University College Dublin, Dublin, Ireland*¹⁹*INFN Sezione di Bari, Bari, Italy*²⁰*INFN Sezione di Bologna, Bologna, Italy*²¹*INFN Sezione di Ferrara, Ferrara, Italy*²²*INFN Sezione di Firenze, Firenze, Italy*²³*INFN Laboratori Nazionali di Frascati, Frascati, Italy*²⁴*INFN Sezione di Genova, Genova, Italy*²⁵*INFN Sezione di Milano, Milano, Italy*²⁶*INFN Sezione di Milano-Bicocca, Milano, Italy*²⁷*INFN Sezione di Cagliari, Monserrato, Italy*²⁸*Università degli Studi di Padova, Università e INFN, Padova, Padova, Italy*²⁹*INFN Sezione di Pisa, Pisa, Italy*³⁰*INFN Sezione di Roma La Sapienza, Roma, Italy*³¹*INFN Sezione di Roma Tor Vergata, Roma, Italy*³²*Nikhef National Institute for Subatomic Physics, Amsterdam, Netherlands*³³*Nikhef National Institute for Subatomic Physics and VU University Amsterdam, Amsterdam, Netherlands*³⁴*AGH—University of Science and Technology, Faculty of Physics and Applied Computer Science, Kraków, Poland*³⁵*Henryk Niewodniczanski Institute of Nuclear Physics Polish Academy of Sciences, Kraków, Poland*³⁶*National Center for Nuclear Research (NCBJ), Warsaw, Poland*³⁷*Horia Hulubei National Institute of Physics and Nuclear Engineering, Bucharest-Magurele, Romania*³⁸*Petersburg Nuclear Physics Institute NRC Kurchatov Institute (PNPI NRC KI), Gatchina, Russia*

- ³⁹Institute for Nuclear Research of the Russian Academy of Sciences (INR RAS), Moscow, Russia
⁴⁰Institute of Nuclear Physics, Moscow State University (SINP MSU), Moscow, Russia
⁴¹Institute of Theoretical and Experimental Physics NRC Kurchatov Institute (ITEP NRC KI), Moscow, Russia
⁴²Yandex School of Data Analysis, Moscow, Russia
⁴³Budker Institute of Nuclear Physics (SB RAS), Novosibirsk, Russia
⁴⁴Institute for High Energy Physics NRC Kurchatov Institute (IHEP NRC KI), Protvino, Russia, Protvino, Russia
⁴⁵ICCUB, Universitat de Barcelona, Barcelona, Spain
⁴⁶Instituto Galego de Física de Altas Enerxías (IGFAE), Universidade de Santiago de Compostela, Santiago de Compostela, Spain
⁴⁷Instituto de Física Corpuscular, Centro Mixto Universidad de Valencia—CSIC, Valencia, Spain
⁴⁸European Organization for Nuclear Research (CERN), Geneva, Switzerland
⁴⁹Institute of Physics, Ecole Polytechnique Fédérale de Lausanne (EPFL), Lausanne, Switzerland
⁵⁰Physik-Institut, Universität Zürich, Zürich, Switzerland
⁵¹NSC Kharkiv Institute of Physics and Technology (NSC KIPT), Kharkiv, Ukraine
⁵²Institute for Nuclear Research of the National Academy of Sciences (KINR), Kyiv, Ukraine
⁵³University of Birmingham, Birmingham, United Kingdom
⁵⁴H.H. Wills Physics Laboratory, University of Bristol, Bristol, United Kingdom
⁵⁵Cavendish Laboratory, University of Cambridge, Cambridge, United Kingdom
⁵⁶Department of Physics, University of Warwick, Coventry, United Kingdom
⁵⁷STFC Rutherford Appleton Laboratory, Didcot, United Kingdom
⁵⁸School of Physics and Astronomy, University of Edinburgh, Edinburgh, United Kingdom
⁵⁹School of Physics and Astronomy, University of Glasgow, Glasgow, United Kingdom
⁶⁰Oliver Lodge Laboratory, University of Liverpool, Liverpool, United Kingdom
⁶¹Imperial College London, London, United Kingdom
⁶²Department of Physics and Astronomy, University of Manchester, Manchester, United Kingdom
⁶³Department of Physics, University of Oxford, Oxford, United Kingdom
⁶⁴Massachusetts Institute of Technology, Cambridge, Massachusetts, USA
⁶⁵University of Cincinnati, Cincinnati, Ohio, USA
⁶⁶University of Maryland, College Park, Maryland, USA
⁶⁷Los Alamos National Laboratory (LANL), Los Alamos, New Mexico, USA
⁶⁸Syracuse University, Syracuse, New York, USA
⁶⁹School of Physics and Astronomy, Monash University, Melbourne, Australia
(associated with Department of Physics, University of Warwick, Coventry, United Kingdom)
⁷⁰Pontifícia Universidade Católica do Rio de Janeiro (PUC-Rio), Rio de Janeiro, Brazil
(associated with Universidade Federal do Rio de Janeiro (UFRJ), Rio de Janeiro, Brazil)
⁷¹Physics and Micro Electronic College, Hunan University, Changsha City, China
(associated with Institute of Particle Physics, Central China Normal University, Wuhan, Hubei, China)
⁷²Guangdong Provincial Key Laboratory of Nuclear Science, Institute of Quantum Matter, South China Normal University, Guangzhou, China (associated with Center for High Energy Physics, Tsinghua University, Beijing, China)
⁷³School of Physics and Technology, Wuhan University, Wuhan, China
(associated with Center for High Energy Physics, Tsinghua University, Beijing, China)
⁷⁴Departamento de Física, Universidad Nacional de Colombia, Bogota, Colombia
(associated with LPNHE, Sorbonne Université, Paris Diderot Sorbonne Paris Cité, CNRS/IN2P3, Paris, France)
⁷⁵Universität Bonn—Helmholtz-Institut für Strahlen und Kernphysik, Bonn, Germany
(associated with Physikalisches Institut, Ruprecht-Karls-Universität Heidelberg, Heidelberg, Germany)
⁷⁶Institut für Physik, Universität Rostock, Rostock, Germany
(associated with Physikalisches Institut, Ruprecht-Karls-Universität Heidelberg, Heidelberg, Germany)
⁷⁷INFN Sezione di Perugia, Perugia, Italy (associated with INFN Sezione di Ferrara, Ferrara, Italy)
⁷⁸Van Swinderen Institute, University of Groningen, Groningen, Netherlands
(associated with Nikhef National Institute for Subatomic Physics, Amsterdam, Netherlands)
⁷⁹Universiteit Maastricht, Maastricht, Netherlands
(associated with Nikhef National Institute for Subatomic Physics, Amsterdam, Netherlands)
⁸⁰National Research Centre Kurchatov Institute, Moscow, Russia
(associated with Institute of Theoretical and Experimental Physics NRC Kurchatov Institute (ITEP NRC KI), Moscow, Russia)
⁸¹National Research University Higher School of Economics, Moscow, Russia
(associated with Yandex School of Data Analysis, Moscow, Russia)
⁸²National University of Science and Technology “MISIS”, Moscow, Russia
(associated with Institute of Theoretical and Experimental Physics NRC Kurchatov Institute (ITEP NRC KI), Moscow, Russia)
⁸³National Research Tomsk Polytechnic University, Tomsk, Russia
(associated with Institute of Theoretical and Experimental Physics NRC Kurchatov Institute (ITEP NRC KI), Moscow, Russia)
⁸⁴DS4DS, La Salle, Universitat Ramon Llull, Barcelona, Spain (associated with ICCUB, Universitat de Barcelona, Barcelona, Spain)

⁸⁵*University of Michigan, Ann Arbor, Michigan, USA (associated with Syracuse University, Syracuse, New York, USA)*

^aAlso at Università di Genova, Genova, Italy.

^bAlso at Università di Bologna, Bologna, Italy.

^cAlso at Università di Modena e Reggio Emilia, Modena, Italy.

^dAlso at Università di Ferrara, Ferrara, Italy.

^eAlso at Università di Milano Bicocca, Milano, Italy.

^fAlso at Università di Bari, Bari, Italy.

^gAlso at Università di Cagliari, Cagliari, Italy.

^hAlso at Novosibirsk State University, Novosibirsk, Russia.

ⁱAlso at Università di Roma Tor Vergata, Roma, Italy.

^jAlso at Universidade Federal do Triângulo Mineiro (UFTM), Uberaba-MG, Brazil.

^kAlso at AGH—University of Science and Technology, Faculty of Computer Science, Electronics and Telecommunications, Kraków, Poland.

^lAlso at Università di Siena, Siena, Italy.

^mAlso at Università di Padova, Padova, Italy.

ⁿAlso at Scuola Normale Superiore, Pisa, Italy.

^oAlso at Università degli Studi di Milano, Milano, Italy.

^pAlso at MSU—Iligan Institute of Technology (MSU-IIT), Iligan, Philippines.

^qAlso at Università di Firenze, Firenze, Italy.

^rAlso at Hanoi University of Science, Hanoi, Vietnam.

^sAlso at P.N. Lebedev Physical Institute, Russian Academy of Science (LPI RAS), Moscow, Russia.

^tAlso at Università di Pisa, Pisa, Italy.

^uAlso at Università della Basilicata, Potenza, Italy.

^vAlso at Università di Urbino, Urbino, Italy.